

STRAIN GAUGE-BASED POSITION MONITORING OF SRF CAVITY

N. Ohm[†], V. Dürr, F. Glöckner, J. Knobloch¹, F. Plocksch, K. Schemmel, A. Velez Saiz², S. Wiese, N. Wunderer, Helmholtz-Zentrum Berlin, Berlin, Germany
¹also at University of Siegen, Siegen, Germany
²also at Technical University Dortmund, Dortmund, Germany

Abstract

The variable pulse-length storage ring (VSR) cavities, featuring protruding waveguides and higher order modes (HOM) absorbers, are designed to be installed as part of the cold string in a spaceframe within a cryogenic vessel. Precise alignment of the cavities during installation and continuous position monitoring during operation are required to prevent damage of other cold string components such as bellows. To achieve this, strain gauges are installed on the rods suspending the cavity within the spaceframe, measuring the superimposed strains.

To validate this approach, assembly tests were conducted, comparing strain gauge measurements with laser tracker data. The results demonstrate that strain gauge-based monitoring enables continuous position tracking of the cavity. Operation within a vacuum vessel at low temperature still needs to be tested.

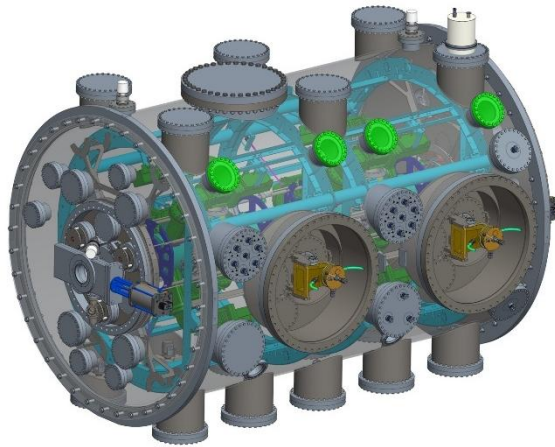


Figure 1: Simplified view of VSR DEMO setup: Cryogenic vessel (transparent grey), ports for laser tracker (light green), spaceframe (light blue), HOM absorber (dark green) and support disc (dark blue) for SRF Cavity.

INTRODUCTION

The VSR DEMO cold string setup consists of two fundamental power couplers (FPCs), each connected to a 1.5 GHz SRF cavity [1]. These two cavities are linked via a collimating shielded bellows (CSB) and require exceptional position stability. This is primarily because the CSB offers limited length compensation, owing to its compact bellows design. Additionally, the FPC extends from outside into the module, connecting both the vessel and the cold string; thus, any positional change of the cavity directly induces misalignment in the FPC. Although bellows are

integrated into the coupler assembly, their ability to compensate for displacement — especially in directions perpendicular to the central axis — is strongly constrained. To prevent damage to these bellows, particularly those on the FPC, it is essential to continuously monitor the cavity's position, especially during thermal transitions such as cool-down and warm-up (see Fig. 1)

MOTIVATION

High-accuracy absolute position measurements can be achieved using laser trackers; however, this technique requires direct visual access to optical targets mounted on the cavity. In the planned configuration, two targets are mounted on each support disc, allowing one laser tracker to trace the corresponding cavity (see Fig. 2).

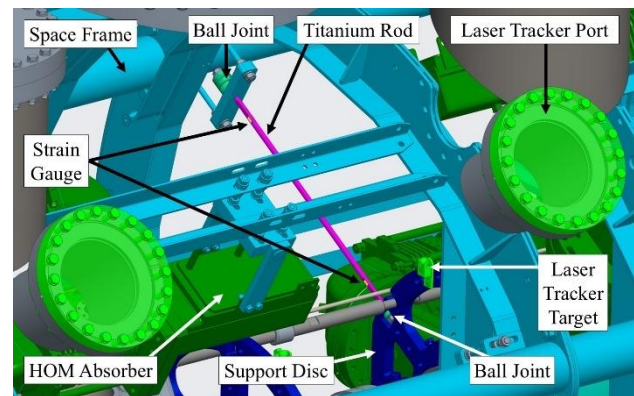


Figure 2: simplified view of VSR DEMO: rods with strain gauges near spaceframe and near support disc, and laser tracker view paths. Cryogenic vessel, magnetic and thermal shields are invisible.

Two trackers are required for both cavities, which are positioned at elevated locations to ensure a clear line of sight in the cryomodule. Refractive-index changes along the optical path, caused by different media (air, glass, vacuum), will be compensated using the Measurement In Different Media Adaptation System (MIDAS) [2]. Ensuring unobstructed sightlines is challenging due to the multiple cold-mass layers — such as thermal shields, multilayer insulation, and piping — and the limited available mounting positions for the targets. Moreover, tracking only two points per support disc prevents full spatial reconstruction of cavity motion, as at least a third point would be required.

The support discs are connected radially to the spaceframe by titanium rods, so that any deformation of the cavities is transferred to these rods as a load change (see Fig. 3).

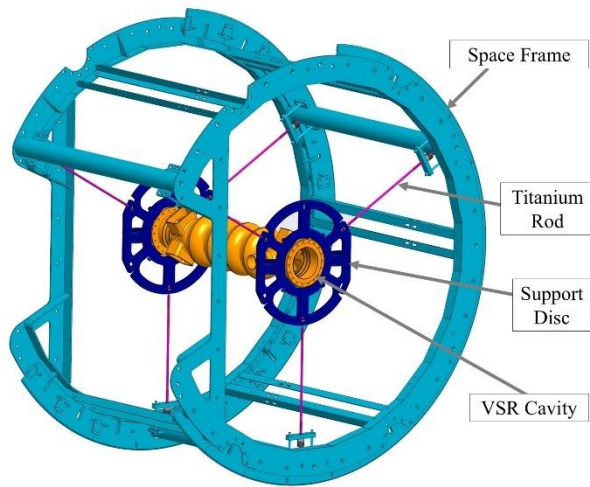


Figure 3: simplified view of mock-up: spaceframe with rods, support discs and cavity dummy. HOM dummies are invisible.

To complement the discrete measurements taken by the laser trackers, we attached strain gauges to these rods to enable continuous monitoring during operation and to detect deformations caused by mechanical loads.

A mock-up installation [3] with a suspended dummy cavity was used to compare strain-gauge signals with laser tracker data. This study provided the basis for evaluating the strain-gauge measurement approach, analysing the influence of gauge location on the titanium rods, investigating rod loading during cavity motion, and assessing the potential to detect cavity displacements.

PREPARE TITANIUM RODS

Each titanium rod is milled close to its ends to create two parallel, flat surfaces. Before installation in the VSR DEMO module, the strain gauges must be applied and calibrated as a Wheatstone bridge. The highest resolution and greatest flexibility would be achieved by using two pairs of strain gauges with grids perpendicular to each other (T-rosettes) on each milled surface (see Fig. 4).

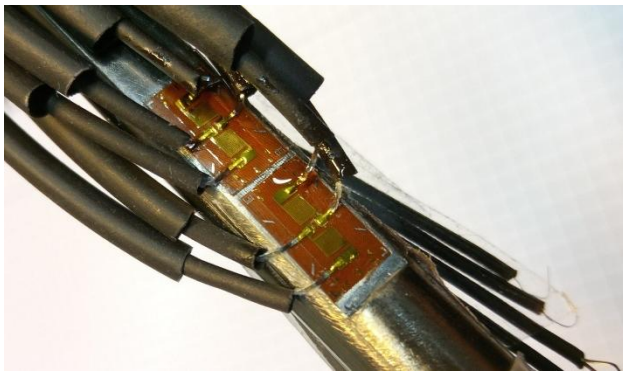


Figure 4: Two T-Rosettes on dummy rod.

However, due to the limited length of the cables, it was decided to use one rosette on each surface, with which pure bending, normal forces and superimposed strain can be determined.

The applied strain gauge configured as Wheatstone bridges for measuring normal stress [4] at both end of the rod. The full-scale value of the normal force measuring range is determined for each bridge using two-point calibration. The expected value for the measuring range end value for normal force on the rod is estimated as follows.

$$F_{n \text{ full max}} = \frac{4 * U_{Dmax}}{2 * (1+\nu) * k * U_{Sense}} * A * E_{Ti5} \quad (1) [4, 5]$$

The first calibration point corresponds to the unloaded state (0 N). For an ideal calibration, the second point would require applying a load equivalent to the maximal operational force on the rod (approximately 5 kN). However, implementing such a load in practice is technically complex; therefore, the second calibration point was instead established with an applied load of 70 N.

MOCK-UP INSTALLATION

Titanium rods with calibrated Wheatstone strain gauge bridges enable the installation of a mock-up (see Fig. 5) [3], whereby tightening the fastening nuts of the titanium rods exerted a normal tensile force of approx. 1.4 kN on all rods (see Fig. 6).

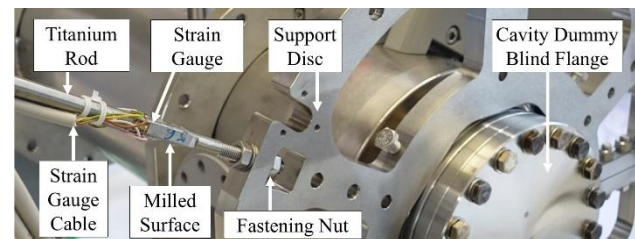


Figure 5: Mock-up with attached cavity.

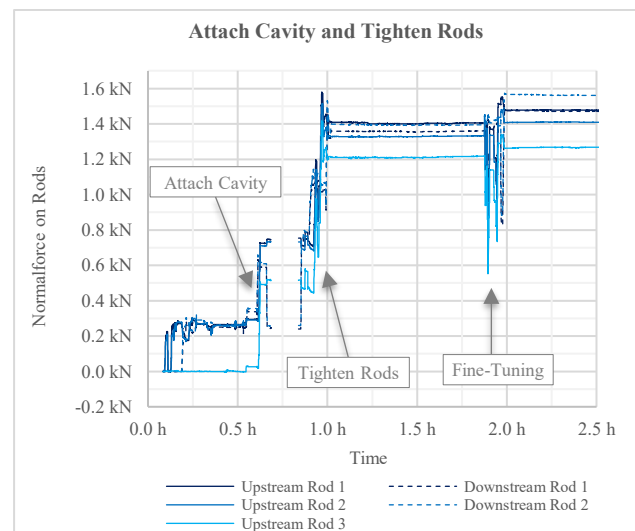


Figure 6: measured normal force on the rods when the cavity is suspended and the rods are tensioned.

After assembly and tightening, the measured values remained stable. After 48 hours the spaceframe was rotated plus/minus 180° for handling purposes [1]. During rotation, the values deviate from the starting value by up to

30%. This indicates movement of the cavity. The cause could be different tensile forces on the rods due to gravity. When the spaceframe returned to its initial position, the force readings deviated by about 2 % from the starting values (see Fig. 7).

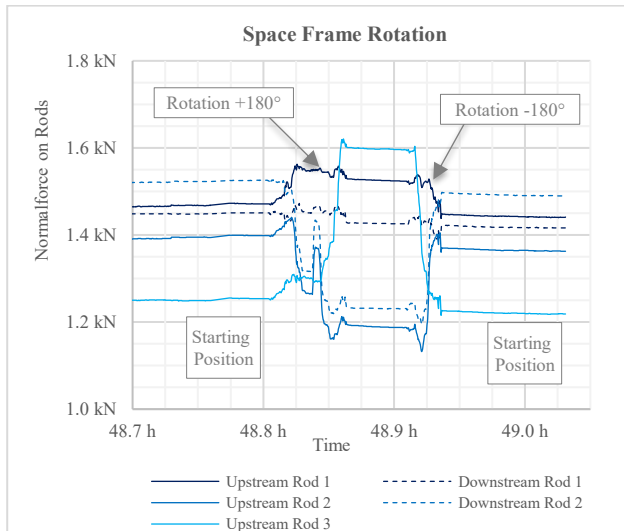


Figure 7: measured normal force on the rods when the space frame is rotated.

MOCK-UP TESTING

For the mock-up tests, an aluminium profile was mounted to the spaceframe in front of the cavity's upstream flange. Using a threaded bracket, a fine adjustment screw applied force near the centre of the blind flange (see Fig. 8). The maximum cavity displacement was limited to 5 mm to prevent damage to the FPC, CSB, and cavity suspension. This displacement value already exceeds the compensation capabilities of the CSB. To determine the resolution of the strain gauge measurement system, the maximal displacement was reached in increments of 0.25 mm each. The force was applied along the central axis of the cavity. The screw was advanced in twenty quarter turns and then retracted in the same manner. To ensure precise and reproducible increments, a mini spirit level was placed on the square head of the screw.

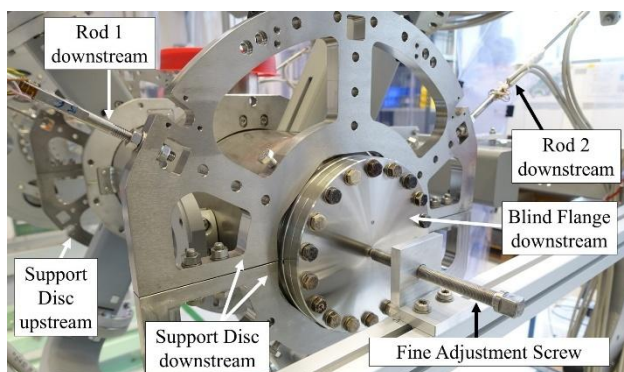


Figure 8: Millimetre screw presses against the flange.

The titanium rods are connected via ball joints at both ends of the cavity suspension, to provide a certain degree of flexibility. It was initially expected that displacement of the cavity would cause all measuring bridges to respond similarly, as if each rod behaved like a beam clamped at one end. This means that the measuring bridges detect bending in the same direction at both ends.

Instead, measurements with the bending full bridges revealed that the section of the rod near the cavity attachment was subjected to bending stress with opposite sign to that at the attachment to the spaceframe, indicating an S-shaped bending profile of the rods (see Fig. 9). When force was applied from the other side, the polarity of the measured bending strains reversed. Because the opposite direction of movement of the cavity causes the S-shaped deformation of the rods to occur in the opposite direction. We assume that friction in the ball joints was too high and hence the rod behaves as if clamped rigidly at both ends, i.e. statically over defined.

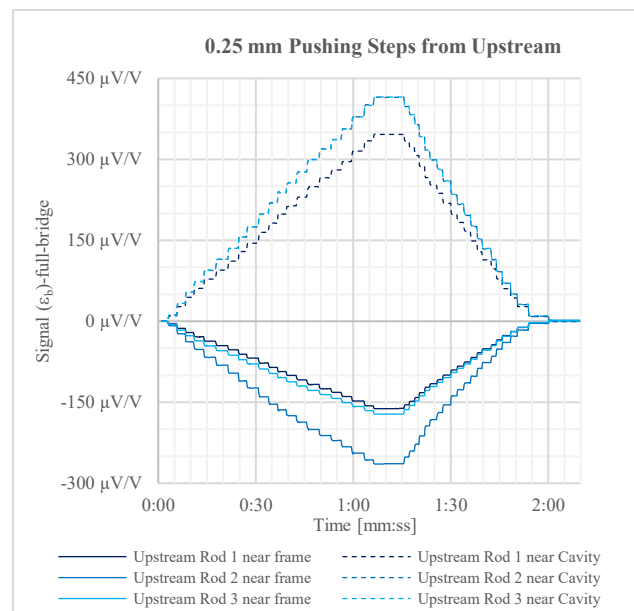


Figure 9: Strain gauge connected as bending measurement bridge. Comparison of strain gauge signal near spaceframe with strain gauge signal near cavity.

Normal force full bridge measurements revealed a different behaviour. When force was applied stepwise from the blind flange upstream side, the downstream side rods relaxed and their measured normal strain remained within the negative range, while the upstream side rods exhibited positive normal strain, reaching a minimum when the screw did not contact the flange (see Fig. 10). Conversely, when force was applied from the downstream side, the upstream side rods relaxed while the downstream rods remained under tensile load. This suggests that the rods are not perfectly parallel to each other and that cavity displacement causes slight pulling of the rods toward the cavity.

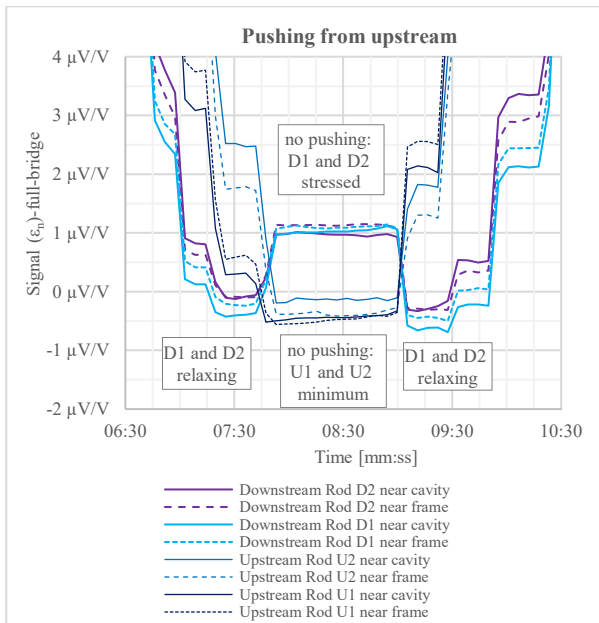


Figure 10: Strain gauge connected as normal measurement bridge. Comparison of the strain gauge signals from downstream side rods with those from the upstream side when pressure is applied from them upstream side.

STRAIN GAUGE VS. LASER TRACKER

The comparison of strain gauge and laser tracker measurements was conducted using the same experimental setup as the mock-up testing. The cavity’s maximum displacement was set to 5 mm by turning the fine-adjustment screw on the downstream support disc in five increments of 1 mm each, applying force directly along the cavity’s central axis consistent with the mock-up test conditions (see Fig. 8).

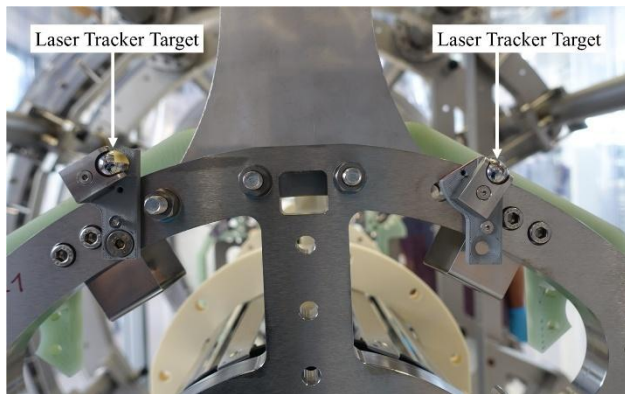


Figure 11: Laser Tracker Targets on cavity support disc.

By measuring distances to reference points on each of the two support discs (see Fig. 11), the laser tracker system determined the spatial position of the cavity relative to the environment (see Fig. 12), with a measurement accuracy of approximately ±0.02 mm. The spaceframe itself was excluded from the tracking. Each measurement series had to be initiated manually, and the data were recorded with corresponding timestamps to ensure temporal correlation.

Meanwhile, eight pairs of strain gauges on four rods were configured as temperature-compensated half-bridges, and their signals were continuously recorded simultaneously by a measurement amplifier throughout the entire measurement process. To measure superimposed load, it is necessary to record the strain on both sides of the milled rod [5].

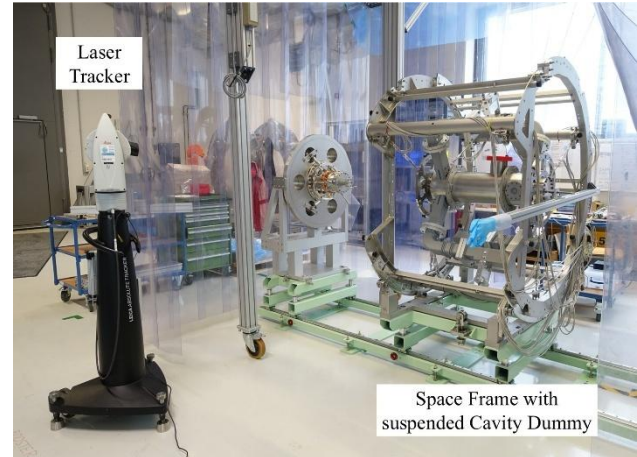


Figure 12: Laser tracker records the position of its targets.

The signals from the measurement bridges show clear steps that correlate with the measured values from the laser trackers (see Fig.13). With an appropriate measuring range, the movement of the cavity can be detected.

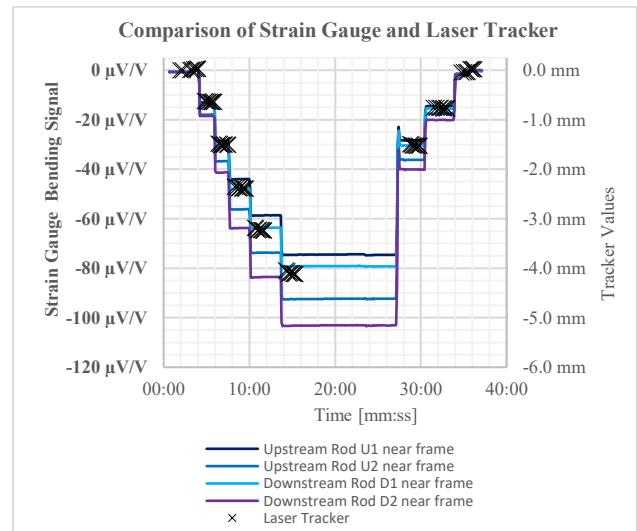


Figure 13: Comparison of strain gauge bending signal with measured values from the laser trackers.

The displacement components perpendicular to the cavity’s central axis, derivable from normal strain via geometric conversions, fell within the laser tracker’s resolution limit and thus could not be independently resolved by the tracker. During the measurement, the room temperature rose by 0.3 °C from 21.6 °C to 21.9 °C, thus remaining almost constant; therefore, any apparent movement in the strain gauge signals due to temperature variation can be disregarded.

Content from this work may be used under the terms of the CC BY 4.0 licence (© 2024). Any distribution of this work must maintain attribution to the author(s), title of the work, publisher, and DOI.

TEMPERATURE DEPENDANCE

Temperature compensation in strain gauges is achieved by matching the thermal expansion coefficient of the gauge material to that of the substrate (e.g., titanium or ferritic steel). Gauges tailored for titanium have a maximum supply voltage of 2.0 V, but the measurement amplifier enforces a constant 2.5 V supply without adjustment options, introducing a risk of self-heating errors. Ferritic steel matched gauges, with slightly different expansion coefficients, tolerate 2.5 V and are less prone to such errors.

Despite the use of temperature compensated half bridges and 6 wire connections to minimise lead resistance effects, measurements still exhibited cyclical variations correlating with ambient temperature. To assess residual thermal influences, a long-term measurement logged both environmental temperature and strain gauge signals.

Without any applied mechanical load, the gauges registered between $-4 \mu\text{V/V}$ and $+3 \mu\text{V/V}$ for a 1°C ambient variation ($20.9\text{--}21.9^\circ\text{C}$), consistent with the theoretical thermal response of titanium for a half bridge configuration (see Fig. 14). The equation of the temperature-compensated half bridge [4] and thermal expansion of titanium [5] result in the theoretical signal titanium expansion $(\varepsilon_n + \varepsilon_b)$ -half-bridge:

$$\frac{U_{D \text{ theo}}(T)}{U_{\text{Sense}}} = 0,25 * (1 + \nu) * k * \alpha * (T - T_0) \quad (2) [4, 5]$$

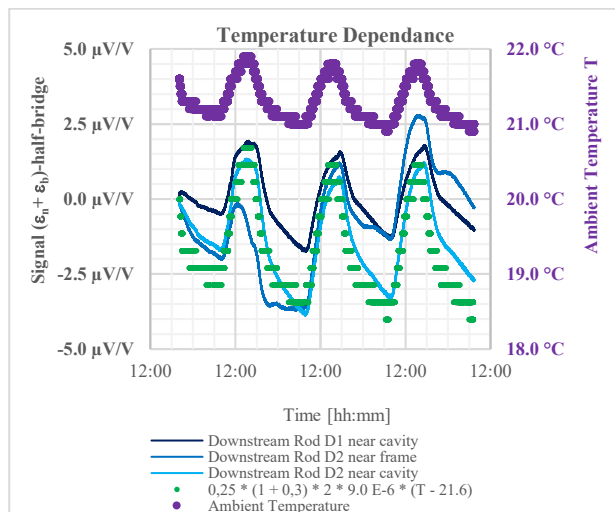


Figure 14: Comparison of a signal temperature compensated half bridges with theoretical thermal response signal of titanium for a half bridge configuration.

The correlation between the bridge signals and the theoretical expected values derived from the temperature change indicates that the bars change length depending on temperature. However, the correlation with the room temperature may be coincidental. Additional unexamined factors include the influence of relative humidity, the absence of gauge covering, and potential adhesive creep or improper strain transfer from the substrate to the gauge grid [6].

CONCLUSION

Comparative testing demonstrated that strain gauges—properly installed, calibrated, and arranged—complement laser tracker measurements well, especially in phases where optical access is unavailable. Laser tracker measurements provide sub 0.1 mm accurate absolute positions, while strain gauges enable continuous, real-time monitoring of cavity displacement and local rod loading without requiring optical access.

Long-term measurements showed minor temperature-related performance fluctuations, which means that calibration under the same climatic conditions as those likely to prevail later in the vessel is necessary to minimise measurement errors caused by temperature influences.

Other environmental and installation-related factors may contribute significantly. For operational use, improved environmental control, sensor protection, and further correlation studies (including humidity effects) are recommended. Further long-term measurements under vacuum conditions and at cryogenic temperatures will test the reliability and accuracy of the system under realistic operating conditions.

Full bridge configurations improve resolution but require more cabling and feed-through that are prone to cause vacuum leaks, while multiple strategically positioned gauges are necessary to interpret superimposed loads. Mock-up tests revealed that strain gauges, depending on placement, orientation and wiring, can detect normal strain, bending, torsion, and their combinations, allowing identification of complex deformation patterns such as S-shaped bending of the support rods under certain loads or parallelism of the rods to be checked.

The method opens new possibilities for recording movements in a cryogenic vessel for improving cavity stability during assembly and thermal cycling by enabling early detection of asymmetries and minimising cool-down misalignments.

REFERENCES

- [1] F. Glöckner *et al.*, “The VSR Demo Module Design -- A Spaceframe-Based Module for Cavities with Warm Waveguide HOM Absorbers”, in *Proc. SRF’21*, East Lansing, MI, USA, Jun.-Jul. 2021, pp. 233.
doi:10.18429/JACoW-SRF2021-MOPTEV013
- [2] V. Velonas, *et al.*, “Measurements with laser tracker through different media: the MIDAS system”, presented at International Workshop on Accelerator Alignment (IWAA) 2018, Batavia, IL, USA, Oct. 2018.
- [3] N. Wanderer, *et al.*, “Mockup assembly of an SRF module: spaceframe as tooling and structural support for highly HOM-damped cavities”, presented at MEDSI’25, Lund, Sweden, Sep. 2025, paper WEP50, unpublished.
- [4] K. Hoffmann, “Anwendung der Wheatstone’schen Brückenschaltung”.
<https://www.hbm.com/de/7163/die-wheatstonesche-brueckenschaltung-kurz-erklart/> [downloaded 02/11/2021]
- [5] K. Gieck and R. Gieck, *Technische Formelsammlung*, 1995. ISBN : 978-3-446-46115-4
- [6] S. Keil, *Dehnungsmessstreifen*, Springer Vieweg, 1995.